Astronomy & Astrophysics

First interstellar detection of OH+

F. Wyrowski, K. M. Menten, R. Güsten, and A. Belloche

Max-Planck-Institut für Radioastronomie, Auf dem Hügel 69, 53121 Bonn, Germany
e-mail: [wyrowski;kmenten;rguesten;belloche]@mpifr-bonn.mpg.de

ABSTRACT

The Atacama Pathfinder Experiment (APEX) 12 m telescope was used to observe the $N = 1-0$, $J = 0-1$ ground-state transitions of OH+ at 909.1588 GHz with the CHAMP+ heterodyne array receiver. Two blended hyperfine structure transitions were detected in absorption against the strong continuum source Sagittarius B2(M) and in several pixels offset by 18″. Both absorption from Galactic center gas and absorption from diffuse clouds in intervening spiral arms in a velocity range from –116 to 38.5 km s^{-1} is observed. The total OH+ column density of absorbing gas is 2.4×10^{15} cm^{-2}. A column density local to Sgr B2(M) of 2.6×10^{14} cm^{-2} is found. On the intervening line-of-sight, the column density per unit velocity interval is in the range of 1 to 40×10^{12} cm^{-2}/(km s^{-1}). OH+ is found to be on average more abundant than other hydrides, such as SH+ and CH+. Abundance ratios of OH and atomic oxygen to OH+ are found in the range of 10^{1-2} and 10^{3-4}, respectively. The detected absorption of a continuous velocity range on the line-of-sight shows OH+ to be an abundant component of diffuse clouds.

Key words. astrochemistry – ISM: abundances – ISM: molecules

1. Introduction

Hydrides are key ingredients of interstellar chemistry since they are the initial products of chemical networks that lead to the formation of more complex molecules. The fundamental rotational transitions of light hydrides fall into the submillimeter wavelength range. A so far elusive but nevertheless important hydride is OH+, oxoniumylidene. OH+ has a $^3\Sigma^-$ ground electric state. Its $N = 1-0$ transition near 1 THz is split into three fine structure components, which are further split into several hyperfine components (Bekooy et al. 1985; Müller et al. 2005).

First estimates of OH+ abundances were given in the calculations of Glassgold & Langer (1976) and Barsuhn & Walmsley (1977). The latter study predicts the highest abundances in low density gas. de Almeida & Singh (1981) conclude that the OH+ molecule is primarily formed in warm, diffuse and moderately thick interstellar clouds. Later de Almeida (1990) discusses the relevance of shocks for the production of OH+ and gives a comprehensive summary of the fine and hyperfine rotational structure and transition probabilities of OH+.

Polehampton et al. (2007) searched for the $N = 2-1$, $J = 1-2$ and $N = 2-1$, $J = 3-2$ transitions at 153.47 and 152.9897 μm, respectively, in the ISO LWS spectrum of Sgr B2 but found a spectral feature at the wavelength of only one of the lines and therefore ruled out a detection of OH+. Also González-Alfonso et al. (2004) discuss an absorption feature in the ISO LWS spectrum of Arp 220 at 153 μm but conclude that it belongs to NH.

A detection of OH+ with the ion mass spectrometer aboard the Giotto spacecraft in the tail of the comet was reported by Balsiger et al. (1986), where OH+ was found to be one of the main cometary hot-ion species in the coma.

OH+ plays an important role also in the formation of water. OH+ is rapidly converted into H_3O^+ which then leads to the formation of water and OH (see e.g. Wannier et al. 1991). This holds in cold and warm environments likewise. Hence, it can either be created via H_3^+ by

$$H_3^+ + O \rightarrow H_2 + OH^+$$
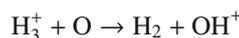
or in warmer regions via H+ with the following two reactions:

$$H^+ + O \rightarrow H + O^+ - k \times 232\,K,$$

$$O^+ + H_2 \rightarrow OH^+ + H.$$
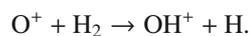
The OH+ then reacts rapidly with molecular hydrogen:

$$OH^+ + H_2 \rightarrow H_2O^+ + H.$$
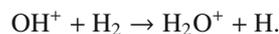
H_2O^+ subsequently reacts with molecular hydrogen to give H_3O^+ which recombines then to form both, OH and water. Therefore measurements of OH+ can provide crucial insight into the part of the oxygen chemical network that leads to the formation of water, which is currently a prominent target for observations with the Herschel Space Observatory. In addition to OH+, several other hydrides (SH+, ^{13}CH+, and HCl) have recently been studied from the ground in the accompanying paper by Menten et al. (2010) in the absorbing diffuse clouds towards Sgr B2(M). This prompted us to also search for OH+and here, we describe the first detection of the OH+ ion in interstellar space using the Atacama Pathfinder Experiment telescope (APEX).
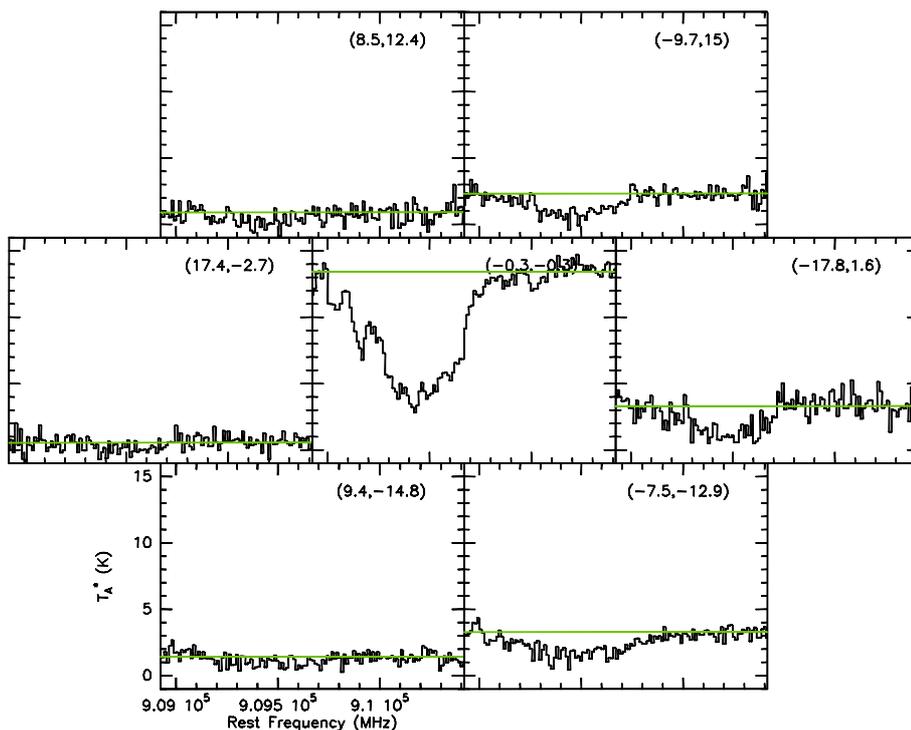
2. Observations and data reduction

The observations were carried out in August 2009 with the the 12-m Atacama Pathfinder Experiment telescope (APEX[1]) (Güsten et al. 2006) using the MPIfR-built CHAMP+ receiver array (Kasemann et al. 2006). The stronger of the two hyperfine lines of the OH$^+$ $N = 1-0$, $J = 0-1$ transition at 909.1588 GHz was tuned into the center of the upper sideband of the high frequency array of the receiver. The array is operated in single sideband mode with a typical rejection of 10db and consists out of seven pixels in a hexagonal pattern with separations of about 18″ and individual beam sizes of 7″. The telescope was pointed towards Sgr B2(M) at a position of α(J2000) = 17^{h}47^{m}20.15^s and δ(J2000) = -28 deg 23′ 04.9″. The SSB system temperatures during the observations were in the range from 10 000 to 20 000 K for the individual pixels with a precipitable water vapor of about 0.6 mm. The relatively high system temperatures are a result of the nearby atmospheric water absorption at 916 GHz. As backends, MPIfR Fast Fourier Transform spectrometers (Klein et al. 2006) were used to cover a bandwidths of 2×1.5 GHz for each pixel with a velocity resolution of 0.25 km s^{-1} that was later lowered to 2 km s^{-1} to increase the signal-to-noise in the spectra. In the following, only spectra from one FFTS per pixel are discussed to exclude possible platforming effects. The wobbling secondary was chopped with a frequency of 1.5 Hz and a throw of 120″ about the cross elevation axis in a symmetric mode which allows a reliable detection of the source continuum as well. Pointing and focus corrections were determined with cross scans on the source itself. With the online calibration, spectra were calibrated to a T_A^* scale. The conversion to T_{MB} was done using a forward efficiency of 0.95 and a beam efficiency measured on Mars at 809 GHz earlier in the month and then scaled to 0.33 for the OH$^+$ frequency.

Table 1. Parameters of the observed lines of the $N = 1-0$ transition.

$J' \leftarrow J''$	$F' \leftarrow F''$	Frequency (MHz)	g_l	g_u	A (10^{-2} s^{-1})
0 1	1/2 1/2	909045.2	2	2	0.524
0 1	1/2 3/2	909158.8	4	2	1.048

Notes. The frequencies were taken from Bekooy et al. (1985) and the Einstein A coefficients from the Cologne Database for Molecular Spectroscopy (CDMS, Müller et al. 2005). Note that the Einstein A coefficients given by de Almeida (1990) are too high by a factor 1.5.

3. Results

Figure 1 shows the spectra towards Sgr B2(M) observed with the 7 different pixels of the array. The baseline offset in the spectra represents the continuum level of the source at the observed positions and is by far strongest in the center pixel on the source. But even towards offset pixels about 18″ away from the center of the source some continuum is detected. In the center pixel the continuum level is at 40 K, although with a slightly different choice of baseline, values as low as 36 K cannot be excluded (see Fig. 2). The overall strength and morphology of the continuum is comparable to that found in the observations presented in the SH$^+$ analysis of Menten et al. (2010). While the absorption from OH$^+$ is most clearly seen towards the center, it is also evident in some of the offset pixels, with a smaller signal-to-noise though, showing that the OH$^+$ absorption is spatially resolved.

The spectrum towards the center pixel is also shown in Fig. 2. Here the frequencies of the two hyperfine lines, which are given in Table 1, are indicated (referenced to a velocity of Sgr B2(M) of 64 km s^{-1}) and a velocity scale is given with respect to the frequency of the stronger OH$^+$ component. Velocities of atomic hydrogen velocity components that were measured by Garwood & Dickey (1989) on the line-of-sight towards Sgr B2(M) are indicated for comparison.
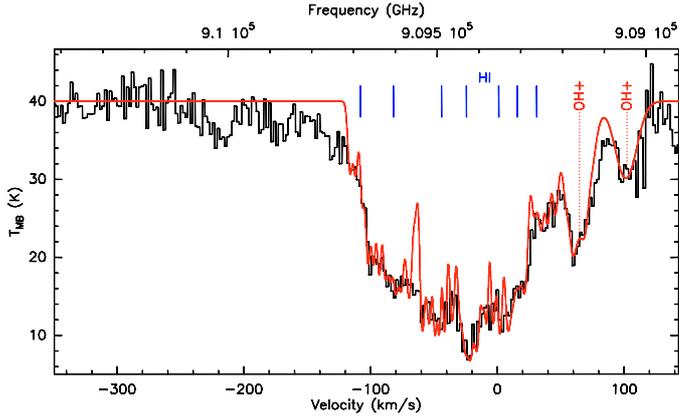
Fig. 2. Observed OH+ spectrum towards Sgr B2(M) in black with the velocity scale referred to the stronger hyperfine line of OH+. Frequencies for the two HFS lines at a velocity of 64 km s^{-1} local to Sgr B2(M) are indicated. Also velocities of the HI components from Garwood & Dickey (1989) are marked. The result from the multi-velocity component fit is overlaid in red.

The optical depth of the absorption can be estimated from the line-to-continuum ratio at each velocity as $\tau = -\log(1 - T_{\rm L}/T_{\rm C})$. This leads to typical opacities of 1, going up to 1.5 at a velocity of −20 km s^{-1}. The total, velocity integrated optical depth of the OH+ absorption from both blended hyperfine lines is $\tau\Delta v = 175$ km s^{-1}.

4. Analysis

From the integrated optical depths the total column density of the absorbing OH+ can be computed from (e.g. Comito et al. 2003):

$$N_{\rm T} = \frac{8\pi\nu^3}{A_{\rm ul}c^3}\frac{g_{\rm l}}{g_{\rm u}}\frac{1}{f}\tau\Delta v \qquad (1)$$

Here it is assumed that only the ground state of the molecule is populated. The $A_{\rm ul}$ are given in Table 1 and are based on the electric dipole moment that Werner et al. (1983) obtained from ab initio calculation. f is the fraction of molecules in the corresponding ground state and $g_{\rm l}$ and $g_{\rm u}$ are the statistical weights of the lower and upper levels, respectively. For the stronger of the hyperfine lines, f is 2/3 and 2/3 of the total optical depth is due to this line, so these two factors cancel out. This leads to a total OH+ column density of 2.4×10^{15} cm^{-2}.

Similar to the analysis presented in Menten et al. (2010), a multi-component fit towards the spectra was done using the XCLASS tool (Comito et al. 2005, and references therein), taking also the blending of the two observed OH+ hyperfine lines into account. The background continuum temperature was estimated from the measured continuum offset in the spectrum and the cosmic microwave background temperature was used as the excitation temperature. For a reasonable fit of the OH+ absorption, many more velocity components were necessary than e.g. the ones reported by Garwood & Dickey (1989). We therefore fit the same components that Menten et al. (2010) used for SH+ and ^{13}CH+, which also allows a more consistent comparison of those hydrides with OH+. The result of the fit is shown in Fig. 2 and the fit components are given in Table 2. Since the derived column densities are mostly determined by the observed line-to-continuum ratio, errors in the absolute calibration will not affect the results. Only uncertainties in the baseline level, as discussed

Table 2. OH+ fit results using the velocity components from the SH+ analysis and from Garwood & Dickey (1989).

$V_{\rm lsr}$ (km s^{-1})	ΔV (km s^{-1})	N (10^{12} cm^{-2})
Menten et al. (2010) components:		
64.0	19	257
38.5	5	6
32.0	5	24
22.0	5	44
17.0	5	29
12.0	6	22
8.2	5	88
2.5	5	103
−2.5	4	88
−8.7	5	88
−15.5	6	147
−20.0	5	96
−25.0	6	221
−29.5	4	59
−35.5	4	88
−41.3	3	74
−45.7	3	66
−49.0	3	66
−53.5	4	88
−58.7	4	96
−69.8	6	118
−76.0	4	81
−80.1	4	66
−84.3	5	96
−88.5	4	66
−93.0	4	74
−97.5	4	66
−101.8	4	66
−106.2	4	37
−111.6	4	25
−116.0	4	24
Garwood & Dickey (1989) components:		
−108.0	7	51
−82.0	28	625
−52.0	17	257
−46.0	8	74
−24.4	14	515
1.1	19	441
15.7	7	15
31.0	21	74
52.8	11	44
66.7	16	221
Vastel et al. (2002) components:		
−108.0	7	66
−92.0	14	294
−77.0	14	294
−61.5	7	147
−52.0	8	147
−44.0	8	147
−21.5	15	515
−3.5	12	294
5.5	12	221
31.0	21	59
52.8	11	44
66.7	16	221

in Sect. 3, might change the column densities by about 20%. The velocity components can account for almost all of the OH+ absorption, missing only a few velocity ranges, e.g. at −64 km s^{-1} and maybe at velocities beyond −116 km s^{-1}, depending on the chosen baseline level. In order to compare OH+ column
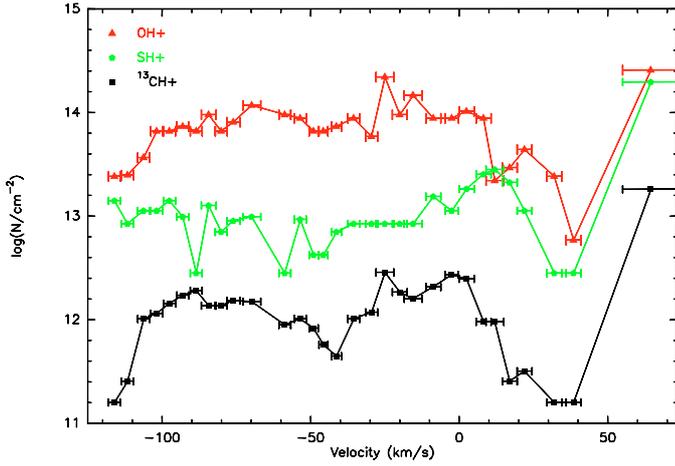
Fig. 3. Comparison of hydride column densities from this work and Menten et al. (2010) as a function of v_{LSR}. The velocity widths of the components are indicated by horizontal bars.
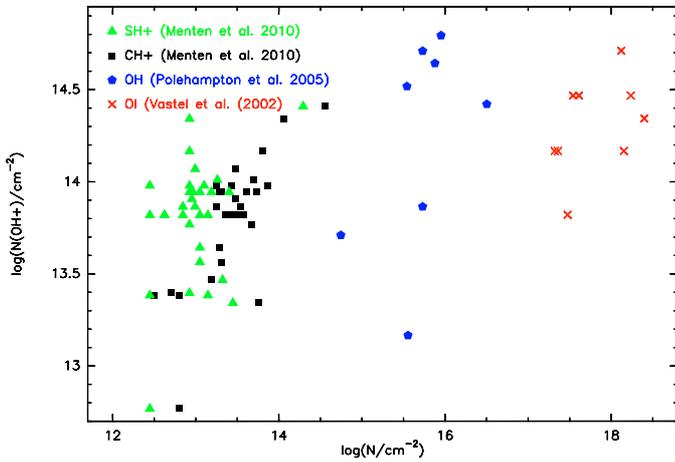
Fig. 4. Correlations of column densities from different molecules with OH$^+$. CH$^+$ column densities were computed from ^{13}CH$^+$ using the isotopic ratios given in Menten et al. (2010). Note, since OH and OI were taken from ISO observations with low velocity resolution, fewer and broader velocity components were used to determine the corresponding OH$^+$ column densities.

Table 3. Median column density ratios and ratio ranges of different molecules with respect to OH$^+$ (Menten et al. 2010; Polehampton et al. 2005; Vastel et al. 2002).

Molecule	$N(X)/N(OH^+)$		
	Min.	Median	Max.
SH$^+$	0.03	0.13	1.28
CH$^+$	0.13	0.43	2.61
OH	10.50	15.83	245.09
OI	1191.42	2587.08	11392.25

were considered since OI turns into emission at larger velocities (Vastel et al. 2002).

5. Discussion and conclusions

Table 3 gives the column density ratios of several molecules with OH$^+$. For SH$^+$ and CH$^+$ the highest ratios are reached towards the Sgr B2(M) local velocity of 64 km s^{-1} but for the rest of the line-of-sight OH$^+$ is more abundant. Ratios to OH and atomic oxygen are found to be in the range of 10^{1-2} and 10^{3-4}, respectively. For velocities between -120 and -10 km s^{-1}, Neufeld et al. (2000) give ortho-water column densities of about 4×10^{15} cm^{-2}, hence the water to OH$^+$ ratio in this velocity range is about 40.

Stäuber et al. (2005) characterize OH$^+$ as a pure X-ray tracer, more likely to be enhanced by X-rays than by FUV radiation but their models for higher density star formation environs cannot reproduce the low OH/OH$^+$ ratio observed here on the Sgr B2(M) line-of-sight. On the other hand, the old Glassgold & Langer (1976) and Barsuhn & Walmsley (1977) studies for low density, diffuse environs predict ratios in agreement with the observed ones. van Dishoeck & Black (1986) emphasize that the formation rates of the simple oxygen-bearing molecules are proportional to the cosmic-ray ionization rate. Their models of diffuse clouds result in typical ratios between OH and OH$^+$ of about 100, as typically found here, but the lines of sight that they model have significantly lower column densities than the Sgr B2(M) intervening clouds.

Optical depths of individual velocity components of OH$^+$ go up to 1.5 meaning that for the other THz lines of OH$^+$ at 972 and 1033 GHz, which are about a factor 4 and 2, respectively, stronger, optical depths will become a problem in the analysis of the column densities. Also the increasing number of hyperfine components will become an issue in the interpretation of absorption of large velocity ranges. For extreme clouds, it might even be feasible to observe the less abundant ^{18}OH$^+$ isotopologue.

The first detection of OH$^+$ presented here, detected by its absorption of a continuous velocity range on the Sgr B2(M) line-of-sight, shows OH$^+$ to be an abundant ingredient of diffuse clouds, even more abundant than published chemical models suggest. Although the 909 GHz line is close to atmospheric water absorption, this detection shows that OH$^+$ can be studied from the ground from excellent sites such as the Chajnantor plateau in Chile, offering a new observational tool to study basic oxygen chemistry in interstellar clouds.

densities also with OH and OI results obtained with the ISO long wavelength spectrometer (Vastel et al. 2002; Polehampton et al. 2005), we did additional OH$^+$ fits using those velocity parameters (see Table 2). The total column densities for the different decompositions are between 2.3 and 2.5×10^{15} cm^{-2}.

The measured OH$^+$ column densities $N(OH^+)$ are shown in Fig. 3 together with SH$^+$ and ^{13}CH$^+$ results (Menten et al. 2010). $N(OH^+)$ is of order 10^{14} cm^{-2} for a large range of velocities and seems to follow more closely the ^{13}CH$^+$ than the SH$^+$ velocity structure. This is seen in more detail in Fig. 4 which shows comparisons of the column densities of several molecules with OH$^+$. Loose correlations are found, the strongest being with CH$^+$ which is surprising since there is no clear chemical link between the two. Interestingly, also for OH and CH a close correlations was recently found in observations of translucent clouds (Weselak et al. 2010). This correlation might be simply due to the fact that both hydrides have a constant ratio to H$_2$. Note that for the comparison with OI only velocities below 10 km s^{-1}

References

Balsiger, H., Altwegg, K., Buhler, F., et al. 1986, Nature, 321, 330

Barsuhn, J., & Walmsley, C. M. 1977, A&A, 54, 345

Bekooy, J. P., Verhoeve, P., Meerts, W. L., & Dymanus, A. 1985, J. Chem. Phys., 82, 3868

Comito, C., Schilke, P., Gerin, M., et al. 2003, A&A, 402, 635

Comito, C., Schilke, P., Phillips, T. G., et al. 2005, ApJS, 156, 127

de Almeida, A. A. 1990, Rev. Mex. Astron. Astrofis., 21, 499

de Almeida, A. A., & Singh, P. D. 1981, A&A, 95, 383

Garwood, R. W., & Dickey, J. M. 1989, ApJ, 338, 841

Glassgold, A. E., & Langer, W. D. 1976, ApJ, 206, 85

González-Alfonso, E., Smith, H. A., Fischer, J., & Cernicharo, J. 2004, ApJ, 613, 247

Güsten, R., Nyman, L. Å., Schilke, P., et al. 2006, A&A, 454, L13

Kasemann, C., Güsten, R., Heyminck, S., et al. 2006, in Society of Photo-Optical Instrumentation Engineers, SPIE Conf. Ser., 6275

Klein, B., Philipp, S. D., Krämer, I., et al. 2006, A&A, 454, L29

Menten, K., Wyrowski, F., Belloche, A., et al. 2010, A&A, submitted

Müller, H. S. P., Schlöder, F., Stutzki, J., & Winnewisser, G. 2005, J. Mol. Struct., 742, 215

Neufeld, D. A., Ashby, M. L. N., Bergin, E. A., et al. 2000, ApJ, 539, L111

Polehampton, E. T., Baluteau, J., & Swinyard, B. M. 2005, A&A, 437, 957

Polehampton, E. T., Baluteau, J., Swinyard, B. M., et al. 2007, MNRAS, 377, 1122

Stäuber, P., Doty, S. D., van Dishoeck, E. F., & Benz, A. O. 2005, A&A, 440, 949

van Dishoeck, E. F., & Black, J. H. 1986, ApJS, 62, 109

Vastel, C., Polehampton, E. T., Baluteau, J., et al. 2002, ApJ, 581, 315

Wannier, P. G., Pagani, L., Kuiper, T. B. H., et al. 1991, ApJ, 377, 171

Werner, H., Rosmus, P., & Reinsch, E. 1983, J. Chem. Phys., 79, 905

Weselak, T., Galazutdinov, G. A., Beletsky, Y., & Krełowski, J. 2010, MNRAS, 402, 1991